Molecular Cell, Vol. 18, 201–212, April 15, 2005, Copyright ©2005 by Elsevier Inc. DOI 10.1016/j.molcel.2005.03.016

Specificity Determinants in Inositol Polyphosphate Synthesis: Crystal Structure of Inositol 1,3,4-Trisphosphate 5/6-Kinase

Gregory J. Miller,[1] Monita P. Wilson,[2] Philip W. Majerus,[2] and James H. Hurley[1,*]
[1]Laboratory of Molecular Biology
National Institute of Diabetes and Digestive and Kidney Diseases
National Institutes of Health
United States Department of Health and Human Services
Bethesda, Maryland 20892
[2]Division of Hematology
Washington University School of Medicine
St. Louis, Missouri 63110

Summary

Inositol hexakisphosphate and other inositol high polyphosphates have diverse and critical roles in eukaryotic regulatory pathways. Inositol 1,3,4-trisphosphate 5/6-kinase catalyzes the rate-limiting step in inositol high polyphosphate synthesis in animals. This multifunctional enzyme also has inositol 3,4,5,6-tetrakisphosphate 1-kinase and other activities. The structure of an archetypal family member, from *Entamoeba histolytica,* has been determined to 1.2 Å resolution in binary and ternary complexes with nucleotide, substrate, and product. The structure reveals an ATP-grasp fold. The inositol ring faces ATP edge-on such that the 5- and 6-hydroxyl groups are nearly equidistant from the ATP γ-phosphate in catalytically productive phosphoacceptor positions and explains the unusual dual site specificity of this kinase. Inositol tris- and tetrakisphosphates interact via three phosphate binding subsites and one solvent-exposed site that could in principle be occupied by 18 different substrates, explaining the mechanisms for the multiple specificities and catalytic activities of this enzyme.

Introduction

The inositol polyphosphates (IPs) are a class of water-soluble signaling molecules derived by phosphorylation of combinations of the six hydroxyl groups on the inositol ring. The manifold possibilities for combinatorial phosphorylation give rise to a large and diverse class of messenger molecules with equally diverse biological roles (Abel et al., 2001; Irvine and Schell, 2001; York et al., 2001). The concept of IPs as messenger molecules arose with the discovery of Ins(1,4,5)P_3 as the initiator of intracellular calcium mobilization (Streb et al., 1983). More recently, inositol hexakisphosphate (IP_6) has come to the fore as a ubiquitous cofactor in many cell processes. IP_6 plays an essential role in DNA repair (Hanakahi et al., 2000; Hanakahi and West, 2002), mRNA export (York et al., 1999), transcriptional regulation (Odom et al., 2000), lymphocyte development (Pouillon et al., 2003), and regulation of chromatin structure (Shen et al., 2003; Steger et al., 2003). Other highly phosphorylated IPs have been reported to regulate exocytosis of insulin granules from pancreatic β cells (Efanov et al., 1997; Hoy et al., 2003; Larsson et al., 1997), phosphoinositide-mediated protein localization (Luo et al., 2003), and ion channels (Kourie et al., 1997). Most recently, the diphosphoinositols IP_7 and IP_8 have been reported to act as high-energy nonenzymatic phosphate donors in protein phosphorylation (Saiardi et al., 2004), and another diphosphoinositol, PP-IP_4, to regulate telomere length (Saiardi et al., 2005; York et al., 2005).

Cellular IP levels are regulated by a chain of phosphorylation and dephosphorylation events (Majerus et al., 1999; Shears, 2004). One of the unusual features of IP metabolism is that many of the enzymes involved carry out more than one reaction (Shears, 2004). IP synthetic pathways are structured differently in yeast, plants, and animals. In most systems examined to date, the synthetic IP pathway begins with the hydrolysis of phosphatidylinositol 4,5-bisphosphate by phospholipase C to produce Ins(1,4,5)P_3. In the yeast *Saccharomyces cerevisiae*, Ins(1,4,5)P_3 is the first substrate for a sequence of IP kinase reactions. The multifunctional kinase Ipk2, whose orthologs are known as IPMK in rat (Saiardi et al., 1999) and Ins(1,3,4,6)P_4 5-kinase (Chang et al., 2002) in human, successively phosphorylates Ins(1,4,5)P_3 on the 6 and then 3 positions, followed by Ipk1 phosphorylation of the 2 position of Ins(1,3,4,5,6)P_5 to produce IP_6 (Odom et al., 2000). In humans and other mammals, Ins(1,4,5)P_3 is first phosphorylated by Ins(1,4,5)P_3 3-kinase to produce Ins(1,3,4,5)P_4. Ins(1,3,4,5)P_4 is then dephosphorylated by an IP 5-phosphatase to produce Ins(1,3,4)P_3. Ins(1,3,4)P_3 is the major substrate for Ins (1,3,4) P_3 5/6-kinase (IP56K). IP56K generates both Ins(1,3,4,5)P_4 and Ins(1,3,4,6)P_4, and the latter is the key entry point to the synthesis of all other tetrakis and higher inositol polyphosphates in animals (Verbsky et al., 2005). IP56K is the rate-limiting enzyme in the synthesis of the highly phosphorylated forms of inositol in humans (Verbsky et al., 2005).

In addition to the reactions for which it is named, IP56K phosphorylates Ins(3,4,5,6)P_4 at the 1 position to Ins(1,3,4,5,6)P_5 (Tan et al., 1997; Yang et al., 1999). This reaction is thought to have regulatory importance, since Ins(3,4,5,6)P_4 is an inhibitor of plasma membrane Ca^{2+}-activated Cl^- channels, but Ins(1,3,4,5,6)P_5 is not. Furthermore, IP56K can act as an IP phosphatase in a reaction that requires the presence of Mg^{2+} and a nucleotide. IP56K can dephosphorylate Ins(1,3,4,5)P_4 and Ins(1,3,4,6)P_4 to Ins(1,3,4)P_3, and Ins(1,3,4,5,6)P_5 to Ins(3,4,5,6)P_4 (Ho et al., 2002); reviewed by (Michell, 2002). IP56K can interconvert the IP_4 isomers Ins(1,3,4,5)P_4 and Ins(1,3,4,6)P_4. IP56K has also been linked to protein kinase activity, although the precise nature of the association is unknown (Wilson et al., 2001).

The primary structures of IP56K orthologs share strong sequence homology with each other, but are

*Correspondence: jh8e@nih.gov

only weakly related to other proteins. IP56K has been predicted to be an ATP-grasp family member based on sequence analysis (Cheek et al., 2002). ATP-grasp proteins were described as a family of enzymes that catalyzed ATP-dependent carboxylate-amine and thiol ligase activities (Artymiuk et al., 1996; Fan et al., 1995; Galperin and Koonin, 1997), although additional roles have been discovered for this family subsequently. The pairwise sequence identity to ATP-grasp proteins of known structure is no greater than 13%, and there has been no experimental confirmation of this prediction.

Despite intense interest in IP signaling and progress in characterizing the enzymes and pathways responsible, little is known about the structural mechanisms for specificity, regulation, and catalysis in this system. To date, only one other inositol phosphate kinase structure has been determined, that of Ins(1,4,5)P_3 3-kinase (IP3K). IP3K is structurally related to both protein and lipid kinases despite the lack of primary sequence similarity (Gonzalez et al., 2004; Miller and Hurley, 2004). To begin to fill in the gaps in structural information, we sought to determine the structure of a representative member of this family. The IP56K from *Entamoeba histolytica* (Field et al., 2000) was found to be eminently tractable for atomic-level structural analysis, leading to crystals of catalytically relevant complexes that diffract to up to 1.2 Å resolution. The structure of the IP56K reveals that it has a fold and specificity determinants that are completely different from IP3K and other members of the eukaryotic protein and lipid kinase superfamily. Given the high level of sequence similarity between the enzymes, and the importance of understanding the structural basis of human IP metabolism, the structure of the *E. histolytica* enzyme was used to model that of the human enzyme. This model was used as a basis for mutational analysis of the function of human IP56K.

Results

Overall Structure

The structure of the full-length *E. histolytica* IP56K (residues 1–319) was determined by combining two multiwavelength anomalous dispersion (MAD) data sets, one from crystals soaked in $HgCl_2$, and another from $Sm(OAc)_3$ cocrystals (Figure 1A, Table 1). The entire protein sequence was traceable except for the N- and C-terminal 4 residues, which were not visible in the electron density and are presumed to be disordered. There is a single *E. histolytica* IP56K molecule in the asymmetric unit, consistent with our finding that IP56K is a monomer in solution (data not shown).

IP56K has a globular fold with three domains surrounding a cleft: a primarily N-terminal domain (residues 5–92 and 298–311), a central domain (residues 93–177 and 193–239), and a C-terminal domain (residues 178–192 and 240–297) that together bind a single ATP between them (Figure 1B). Each domain has a core β sheet surrounded by helices. The N-terminal domain consists of a mostly parallel 5-stranded β sheet with a single antiparallel strand (strand 2), and has strand order 5-4-1-3-2 (Figures 1C and 2A). The C-terminal 14 residues comprise an α-helix which forms part of the outer helical shell of the N-terminal domain. The β sheet of the central domain is an antiparallel 5-stranded sheet with strand order 6-9-7-8-12. The β sheet of the C-terminal domain is an antiparallel 4-stranded sheet with strand order 13-14-10-11. The β sheet of the C-terminal domain forms the bottom of the catalytic cleft.

ATP and Mg^{2+} Binding Sites

The structures of the enzyme occupied by several combinations of substrates and products were solved: ADP and Mg^{2+}; AMPPCP, Mg^{2+}, and Ins(1,3,4)P_3; and ADP, Mg^{2+}, and Ins(1,3,4,6)P_4 (Figure 1A). ADP binds in a deep cleft formed by the β sheets of the central and C-terminal domains, which envelop the nucleotide almost entirely and leave only 22% of the ADP exposed to solvent (Figure 2B). The nucleotide binding pocket is walled by many hydrophobic residues, including Pro-109, Ile-134, Tyr-170, Ile-171, Leu-195, Phe-208, and Ile-277. The imidazole ring of His-173 also contributes to the wall. His-173 does not hydrogen bond directly to the adenine but appears to play a critical role in structuring the adenine binding site through its close hydrogen bonds with Ser-194 and the main-chain carbonyl of Ile-171. The major polar contacts between IP56K and the nucleotide include hydrogen bonds of adenine N_6 to Gln-168 and the main-chain O of His-169; adenine N_7 to the Nζ of Lys-136; and the N_1 position to the main-chain NH of Ile-171. The 2′ hydroxyl of the ribose forms a hydrogen bond with Ser-194.

In the absence of bound IP, only one magnesium atom (Mg1) is visible in the density, which is coordinated by Asp-275, Asp-289, oxygen atoms from both the α- and β-phosphates of ADP and two well-ordered water molecules, w1 and w2 (Figure 3A). In the Ins(1,3,4)P_3-bound structure, a second magnesium atom (Mg2) is bound and coordinated by Asp-289, Asn-291, the β-phosphate of ADP and two water molecules, w3 and w4 (Figures 3B and 3E). One of the water molecules, w3, forms a bridge to the 5-hydroxyl of Ins(1,3,4)P_3. In the Ins(1,3,4,6)P_4-bound structure, w3 forms an additional hydrogen bond with an oxygen of the 6-phosphate group (Figures 3C and 3F).

IP Binding Site

The Ins(1,3,4)P_3-bound form shows a network of hydrogen bonds and salt bridges through the 1, 3, and 4-phosphate groups (Figure 3B). The 1-phosphate is hydrogen bonded to the side chains of Lys-179, Arg-192, and Ser-295 and to the main chain NH of Ser-295. The 3-phosphate is hydrogen bonded to the Nζ atoms of the side chains of Lys-17 and Lys-57. The 4-phosphate is hydrogen bonded to the Nζ of Lys-57, the Nϵ of Gln-141, the Nϵ of His-147, and the main chain NH of Gly-142. Gly-142 has (ϕ,ψ) values of 98 and 11 degrees, which would be unusual for any residue other than Gly. None of the free hydroxyl groups at positions 2, 5 or 6 have any direct contact with the enzyme. The bound Ins(1,3,4,6)P_4 is oriented similarly to the Ins(1,3,4)P_3 in the active site, and the 1, 3, and 4-phosphate groups form nearly identical contacts with the enzyme (Figure 3C). Arg-192 moves slightly farther away from the bound product in this structure, as compared to its position in the substrate-bound structure. The 6-phos-

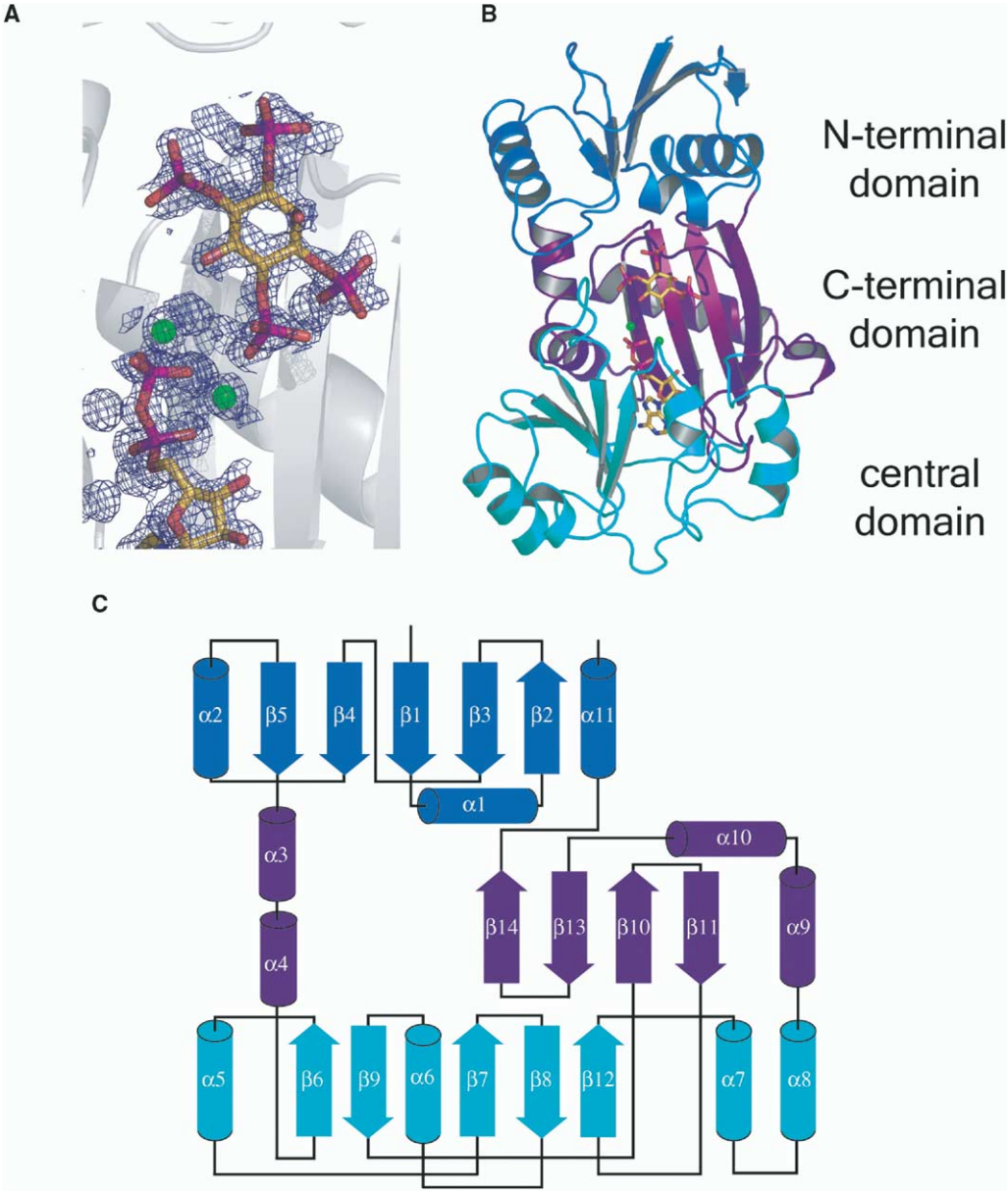

Figure 1. Structure of IP56K

(A) Ins(1,3,4,6)P_4 binding site as defined by an F_o–F_c difference map contoured to 2.0 σ around the IP56K active site demonstrating the location of the bound substrate. F_o was obtained from the Hg λ3 data set obtained from cocrystals of Ins(1,3,4,6)P_4, ADP, and magnesium soaked in $HgCl_2$. F_c was obtained from a partially refined model automatically build with ARP/wARP prior to inclusion of any ligands. Atoms are colored orange (carbon), red (oxygen), blue (nitrogen), green (magnesium), and magenta (phosphorous).

(B) Overall structure of the IP56K monomer. The N-terminal domain is colored blue, the central domain cyan, and the C-terminal domain purple.

(C) Topology diagram of the IP56K, colored as in (B).

phate of Ins(1,3,4,6)P_4 interacts with the Nζ of Lys-179 and the Nδ of Asn-291.

The structures determined from crystals soaked in Ins(1,3,4,5)P_4 revealed electron density for Ins(1,3,4,6)P_4, rather than Ins(1,3,4,5)P_4. The appearance of this species indicates that the enzyme is active for the interconversion of the 5- and 6-phosphates in the presence of ADP in the crystallization medium, as described previously in solution (Ho et al., 2002).

IP56K Is a Member of the ATP-Grasp Family

A comparison of the IP56K to other known structures was performed using the Dali server (Holm and Sander, 1995). The highest 15 scoring entries in the PDB belong to the ATP-grasp domain family (Artymiuk et al., 1996; Fan et al., 1995; Galperin and Koonin, 1997). This family was first defined by the structural similarity between the cell wall synthesis enzyme D-ala-D-ala ligase (Ddl) and glutathione synthetase (GSHase) (Fan et al., 1995).

Table 1. Crystallographic Data and Refinement

Data Set	Sm	Sm	Hg	Hg	Hg	Hg	Native 1	Native 2	Native 3
	λ1	λ2	λ1	λ2	λ3	λ4	ADP	Ins (1,3,4)P_3 + AMPPCP	Ins(1,3,4,6)P_4 + ADP
Data Collection									
Wavelength (Å)	1.8997	1.8453	0.9687	1.0095	1.007	1.008	1.000	1.000	1.000
Unique reflections	14012	13870	22499	20004	19680	19785	91950	86414	86579
Resolution range (Å)	50–2.29	50–2.3	30–2.3	50–2.04	50–2.03	50–2.03	47–1.20	50–1.22	50–1.24
Completeness[a] (%)	98.3 (95.6)	98.3 (94.9)	94.2 (92.4)	99.5 (96.7)	97.1 (95.6)	95.3 (97.7)	94.8 (99.4)	95.9 (93.7)	98.6 (98.0)
R_{merge}[a,b]	0.110 (0.219)	0.095 (0.320)	0.051 (0.075)	0.065 (0.174)	0.080 (0.174)	0.074 (0.098)	0.047 (0.246)	0.034 (0.178)	0.050 (0.286)
Refinement									
$R_{working}$[a,c]							0.182 (0.213)	0.186 (0.210)	0.189 (0.190)
R_{free}[a,d]							0.205 (0.238)	0.209 (0.210)	0.208 (0.225)
R.m.s. deviations:									
Bond length (Å)							0.007	0.007	0.007
Bond angle							1.201	1.237	1.233
B factor (Å^2) main chain							0.426	0.422	0.455
B factor (Å^2) side chain							1.111	1.236	1.266
<B> factor (Å^2) protein							14.555	14.062	13.243
<B> factor (Å^2) ligands							8.803	32.005	14.495
<B> factor (Å^2) solvent							27.388	24.292	25.177
Protein atoms, number							2505	2505	2505
Solvent atoms, number							569	447	552
Ligand atoms, number							26	56	56
Residues in most favored Φ-ψ region							91.5 %	91.5 %	91.5 %

[a] Data in parentheses are for highest resolution shells.
[b] $R_{sym} = \Sigma_h\Sigma_i|I_i(h) - < I(h) > |/\Sigma_h\Sigma_i I_i(h)$.
[c] $R = \Sigma (|F_{obs}| - k|F_{calc}|) / \Sigma|F_{obs}|$.
[d] R_{free} is the R value calculated for a test set of reflections, comprising a randomly selected 5% of the data that is not used during refinement.

The top scoring matches were to the lysine biosynthesis enzyme LysX (rmsd of 2.8 Å over 220 Cα atoms) (Sakai et al., 2003), Ddl (rmsd 3.8 Å over 238 Cα atoms) (Fan et al., 1994), and synapsin Ia (rmsd 3.4 Å over 228 Cα atoms) (Esser et al., 1998). All three domains of IP56K are structurally similar to other ATP-grasp fold proteins (Figures 4A and 4B). This places IP56K in a subset of ATP-grasp proteins with the highest similarity to each other in all three domains: GSHase, Ddl, synapsin Ia, LysX, N^5-carboxyaminoimidazole ribonucleotide synthetase (Thoden et al., 1999), and PurT-encoded glycinamide ribonucleotide transformylase (Thoden et al., 2000). There is only one kinase in the top 78 matches: the ATP-grasp protein pyruvate phosphate dikinase (rmsd 3.2 Å over 169 Cα atoms), which is only similar in two out of three domains (Herzberg et al., 1996). All ATP-grasp proteins bind ATP in a cleft between the β sheets of the central and C-terminal domain.

Thirteen fingerprint residues have been identified as characteristic of the ATP-grasp fold, and nine of these are conserved in IP56K. Two basic residues bind the α- and β-phosphates of ATP, and the more C-terminal of the two also interacts with the ATP adenine N_7. Arg-94 and Lys-136 have these roles in IP56K. A conserved Glu or Gln accepts a hydrogen bond from the adenine N_6, and Gln-168 has this role in IP56K. Tyr-170, Ile-171, and Val-288 take on the roles of conserved hydrophobic residues that bind the face of the adenine ring. The Mg^{2+} binding sites in the ATP-grasp proteins consist of a triad of residues, typically two acidic residues and an Asn (Figure 4D). In IP56K these are Asp-275, Asp-289, and Asn-291 (Figure 4C).

The subset of the most similar ATP-grasp proteins contain a very unusual non-Pro *cis* peptide bond in their N-terminal domain. This is usually an Asn. It is outside of the active site and seems to play a role in stabilizing an unusual tight U-shaped bend in the main chain. Given the high resolution of the structure determination, there is no doubt that Glu-83 is in a *cis* conformation and plays this role in IP56K. This structural similarity further highlights the close relationship of IP56K to other ATP-grasp proteins.

Mutational Analysis of Enzyme Activity

In order to assess the general implications for the enzymatic mechanism of IP56K across species lines, and to test the quality of the comparative model for human IP56K (Figure 2C), thirteen active site residues were mutated in human IP56K. The mutant proteins were expressed in insect cells and their Ins(1,3,4)P_3 5/6-kinase activities determined (Table 2). Mutation of residues coordinating the catalytic Mg^{2+} ions, corresponding to Asp-289 and Asn-291 in *E. histolytica*, led to the most drastic effects. D295A and N297L had no detectable activity, while N297A had activity reduced by more than 10^3-fold. Seven IP phosphate binding residues were mutated: Lys-18, Lys-59, His-162, Gly-163, His-167, Lys-199, and Arg-212, which correspond to Lys-17, Lys-57, Gln-141, Gly-142, His-147, Lys-179, and Arg-192 in *E. histolytica* IP56K. All of the mutants have sharply reduced activity. The largest decrease, by a factor of 2×10^4, was seen for G163P, which blocks the hydrogen bond between the main-chain NH group of the Gly and the 4-phosphate, and probably distorts the conformation of the main chain in this region as well. A

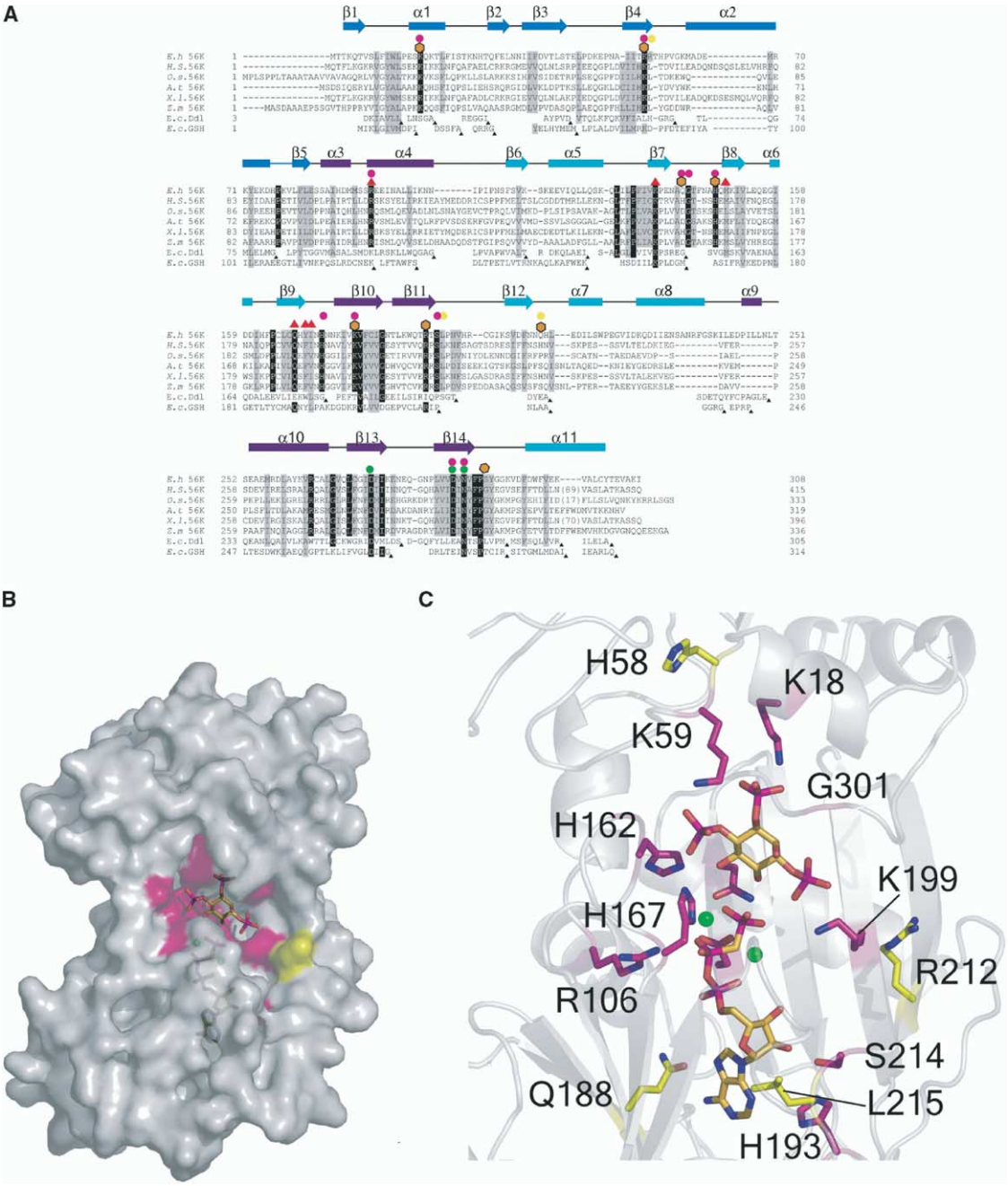

Figure 2. Homology and Alignment of IP56Ks

(A) IP56Ks from *E. histolytica, H. sapiens, O. sativa, A. thaliana, X. laeveis, Z. mays*, and the *E. coli* ATP-grasp proteins Ddl and glutathione synthase. Residues identical across IP56K sequences are boxed in solid black and those that are similar are boxed in gray. Residues that contact the ADP are marked with red triangles, those that contact the IP are marked with orange hexagons and those that coordinate magnesium are marked with green circles. Mutations that reduce activity by more than 100-fold are marked with magenta circles, and mutations the cause lesser reductions in activity are marked with yellow circles. Secondary structure elements of the domains are colored as in Figure 1B. The sites of sequence insertions in other ATP-grasp proteins are shown with black triangles.

(B) Surface diagram of comparative model of human IP56K, with the locations of activity-altering mutants highlighted in the same colors as in (A).

(C) Active site of human IP56K, showing AMPPCP, Ins(1,3,4)P_3, and Mg^{2+} ions. Ligand atoms are colored orange (carbon), red (oxygen), blue (nitrogen), magenta (phosphorous), green (magnesium). Protein carbon atoms are colored yellow or magenta depending on the effect of the corresponding mutation on activity as in (A), and protein oxygen and nitrogen atoms are colored red and blue, respectively.

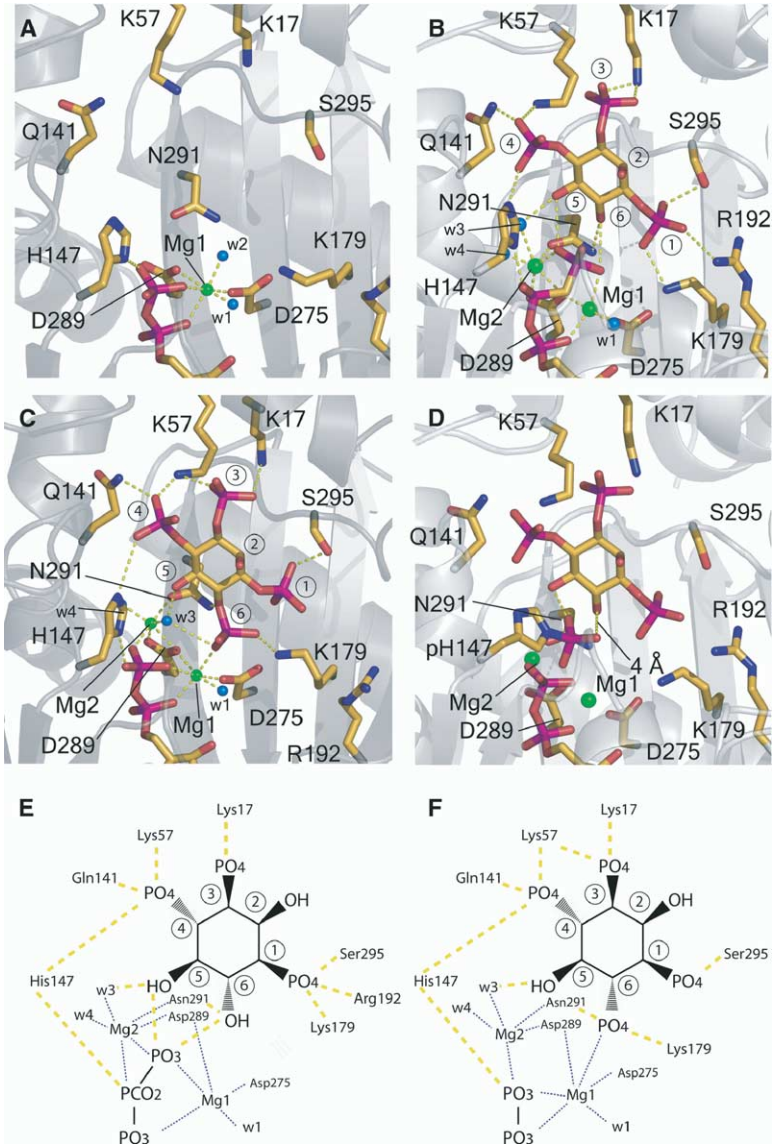

Figure 3. Active Site of IP56K

(A) The ADP complex. Atoms are colored as in Figure 2C. Hydrogen bonds are colored yellow.

(B) AMPPPCP and Ins(1,3,4)P_3 complex.

(C) ADP and Ins(1,3,4,6)P_4 complex.

(D) Model for a hypothetical phosphohistidine intermediate in complex with Ins(1,3,4)P_3 and ADP.

(E) Schematic drawing of the IP56K active site corresponding to the pseudosubstrate complex shown in (B).

(F) Schematic drawing corresponding to the product complex shown in in (C).

large 10^4-fold effect is also seen for H167Q, which is consistent with the intimate involvement of this absolutely conserved His in catalysis. The most modest effects were reductions of the order of 10^2, for K59A and R212A. These lesser effects are consistent with the higher degree of solvent exposure of these two compared to other IP binding residues.

Mutational effects in the ATP binding site were more variable. Mutation of Arg-106, which corresponds to the *E. histolytica* ATP α-phosphate binding Arg-94, reduces activity sharply to 0.06% of wild-type. Mutation of the ribose hydroxyl binding Ser-214 reduces activity to 0.4% of wild-type. On the other hand, two of the residues that interact with the adenine base appear to be nearly dispensable. Mutation of Gln-188 and Leu-215, which correspond to *E. histolytica* Gln-168 and Leu-195, lead to almost negligible reductions in activity. A third mutation in the adenine binding site, H193A, corresponding to *E. histolytica* His-173, reduces activity to 0.3% of wild-type.

The human and *E. histolytica* enzymes produce different ratios of Ins(1,3,4,5)P_4 to Ins(1,3,4,6)P_4. Two mutations were designed to test the origins of product specificity differences between the two species. The H162Q and G301S mutants of the human enzyme shift the ratios to be more like those of the *E. histolytica* enzyme than the wild-type human enzyme (data not shown). The *E. histolytica* enzyme is capable of phosphorylating Ins(1,4,5)P_3 at the 3 position, while the human enzyme cannot except under extreme, nonphysiological conditions. Human Gly-301 corresponds to Ser-295 in *E. histolytica* IP56K. Ser-295 hydrogen bonds to the 1-phosphate of Ins(1,3,4)P_3 and along with Gln-141 are the only direct IP binding residues not conserved between the two species. G301S has sharply reduced activity (Table 2), which we cannot fully account for given the limitations of the comparative model of the human IP56K structure. The Ins(1,4,5)P_3 3-kinase activities of the human and *E. histolytica* wild-type enzymes and the human G301S were assessed

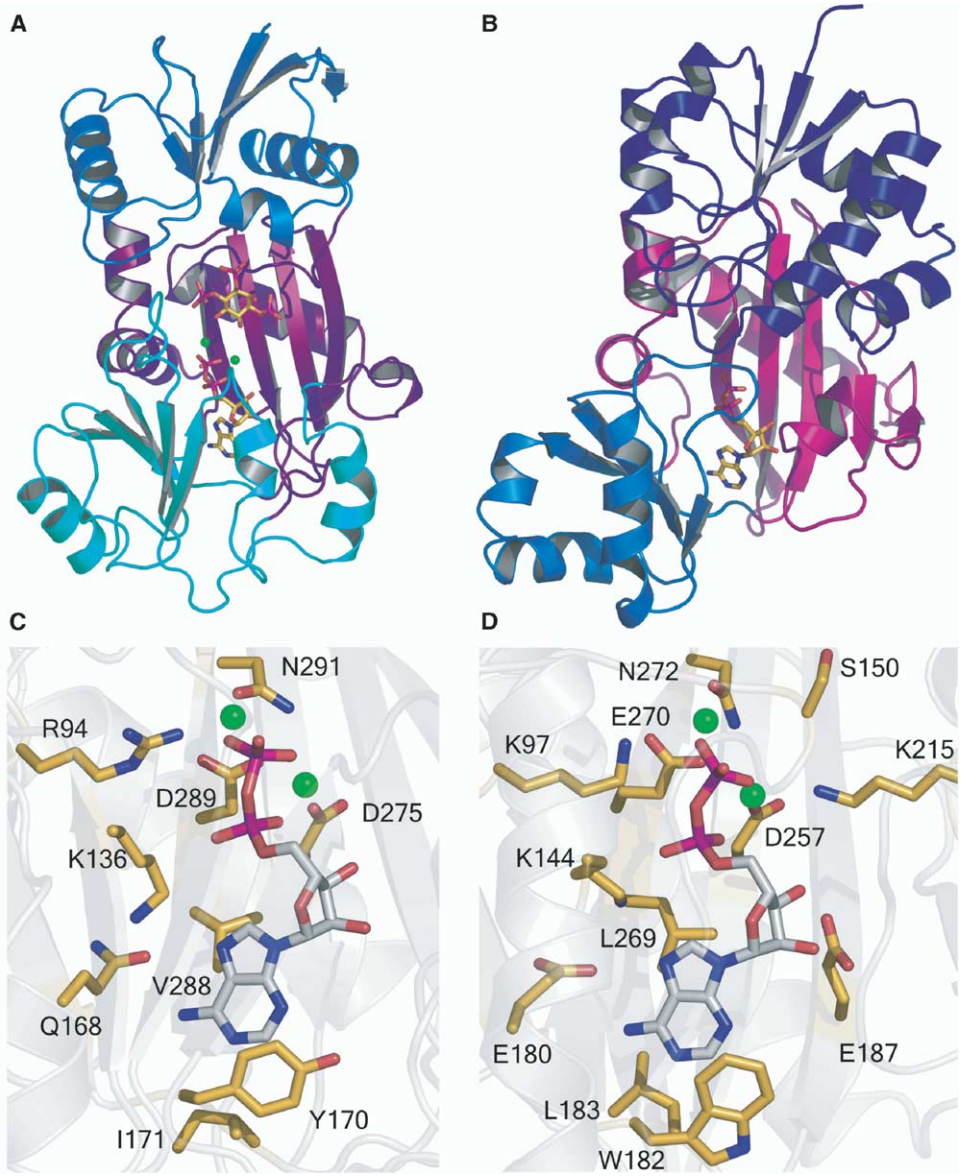

Figure 4. ATP-Grasp Fold of IP56K

(A) Ribbon diagram of IP56K colored as in Figure 1A.

(B) Ribbon diagram of Ddl with the N-terminal domain colored dark blue, the central domain colored light blue, and the C-terminal domain colored pink.

(C) Nucleotide binding site of the IP56K with stick representations of the fingerprint residues of the ATP-grasp family. Atoms are colored as in Figure 2A.

(D) Nucleotide binding site of the Ddl with stick representations of the fingerprint residues of the ATP-grasp family.

(data not shown). G301S produces Ins(1,3,4,5)P_4 from Ins(1,4,5)P_3, like the *E. histolytica* enzyme, but unlike the wild-type human. These data show that the human His-162 and Gly-301 are important determinants for species-specific differences in enzyme properties.

The possible role of human His-167 (*E. histolytica* His-147), which is close enough to the reactive phosphates to suggest a potential role in the isomerization of Ins(1,3,4,5)P_4 to Ins(1,3,4,6)P_4, and vice versa, was tested by assaying the interconversion of these two compounds (Figure 5). The *E. histolytica* enzyme is unable to isomerize Ins(1,3,4,6)P_4 to Ins(1,3,4,5)P_4, although it catalyzes the reverse reaction. Human IP56K mutants H167A, H167Q, N297A, and G301S all behave like the *E. histolytica* enzyme in this respect. The His-167 mutants have almost no detectable activity. Since the kinase activity of His-167 mutants is also sharply reduced, we cannot determine with certainty whether His-167 participates in a covalent intermediate. Structural modeling of a hypothetical phosphohistidine intermediate indicates that without significant conformational changes, the phosphohistidine phosphate would

Table 2. Mutational Analysis of Human IP56K

Human IP56K Site Mutation	Analogous *E. histolytica* Residue	Activity (% wt)	Function of Residue in *E. histolytica*
wt		100	
K18A	K17	0.33	3-phosphate of Ins(1,3,4)P_3
H58A	K57	80	4-phosphate of Ins(1,3,4)P_3
K59A	R58	1.0	Structures inositol phosphate binding loop
R106A	R94	0.06	β-phosphate of AMP-PCP
H162Q	Q141	0.03	4-phosphate of Ins(1,3,4)P_3
G163A	G142	0.90	4-phosphate of Ins(1,3,4)P_3
G163P	G142	0.005	4-phosphate of Ins(1,3,4)P_3
H167A	H147	0.03	4-phosphate of Ins(1,3,4)P3, β-phosphate of AMP-PCP
H167Q	H147	0.01	4-phosphate of Ins(1,3,4)P3, β-phosphate of AMP-PCP
Q188A	Q168	90.0	N_6 of adenine
H193A	H173	0.30	Structures adenine binding site
K199A	K179	0.07	1-phosphate of Ins(1,3,4)P_3, 6-phosphate of Ins(1,3,4,6)P_3
S214A	S194	0.40	2′OH of ribose
R212A	R192	1.2	1-phosphate of Ins(1,3,4)P_3
L215A	L195	75	Hydrophobic nucleotide pocket
D295A	D289	0	Coordination of Mg1 and Mg2
N297A	D291	0.06	Coordination of Mg2, 6-hydroxyl of Ins(1,3,4)P_3
N297L	D291	0	Coordination of Mg2, 6-hydroxyl of Ins(1,3,4)P_3
G301S	S295	0.01	1-phosphate of Ins(1,3,4)P_3

be about 4 Å from the 6-hydroxyl (Figure 3D), too far for efficient transfer. It is clear that His-167 is important for the isomerization reaction, and elucidating its precise role will warrant further investigation.

Discussion

Catalytic Mechanism of the Multifunctional Enzyme IP56K

The crystal structure of the ternary complex of Ins(1,3,4)P_3 and AMPPCP shows that one oxygen of the ATP γ-phosphate approaches the 5-hydroxyl within 2.5 Å, while a different oxygen simultaneously make a similar short-range interaction with the 6-hydroxyl (Figure 3B). The oxygen that approaches that 5-hydroxyl directly coordinates Mg2, while the one that approaches the 6-hydroxyl directly coordinates Mg1. The active site near the 5- and 6-hydroxyls is constricted and therefore could not accommodate more than one phosphate group, consistent with the transfer of a phosphate to either, but never both, of the two hydroxyl groups. The structure shows with striking clarity how

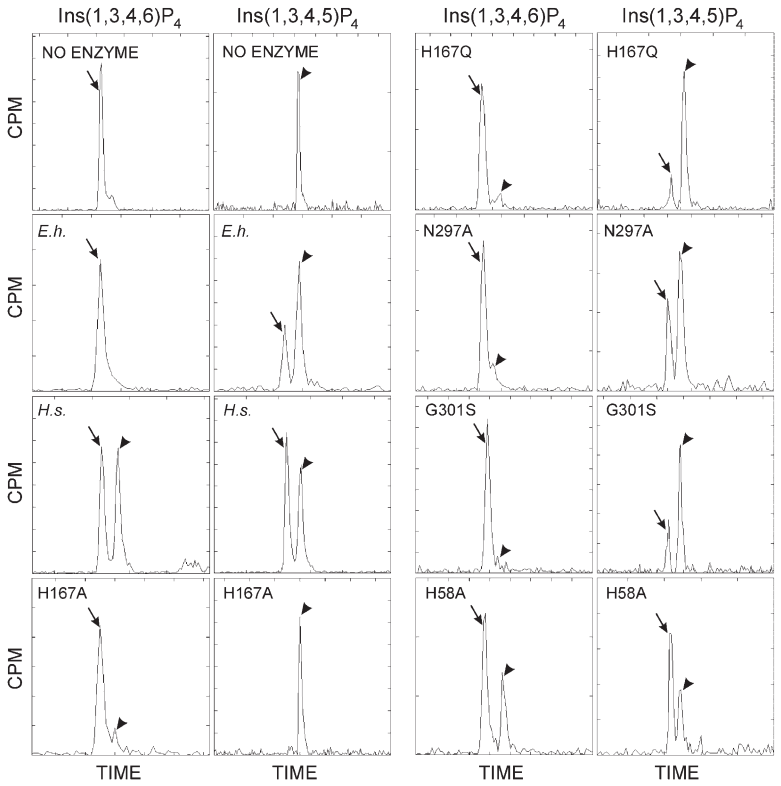

Figure 5. Isomerization Activity of IP56K

Each enzyme preparation (indicated in the upper left corner of each panel) was incubated with 3000 cpm of [^{3}H] Ins(1,3,4,6)P_4 or [^{3}H] Ins(1,3,4,5)P_4 for 3 hr at 37°C (indicated at the top of each panel set). Inositol tetrakisphosphate isomers were then separated using Adsorbosphere SAX HPLC. The elution time for a given inositol polyphosphate isomer depends upon the age of the column, due to degradation of the silica. Therefore, chromatograms are aligned based upon the elution time of the internal standard [^{32}P] Ins(1,3,4,5)P_4. Elution positions of Ins(1,3,4,6)P_4 (arrow) and Ins(1,3,4,5)P_4 (arrowhead) are indicated on each panel. Substrates in the absence of enzyme are shown in the upper left panels. *E.h.* = enzyme from *E. histolytica*. *H.s.* = *H. sapiens*. All mutants are made with the *H.s.* template.

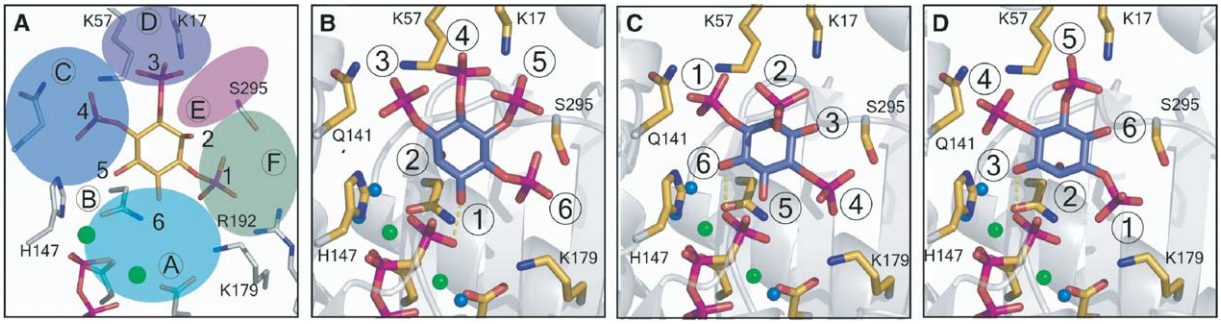

Figure 6. Orientation of Inositol Phosphates in the IP56K Active Site

IP56K kinase reaction substrates.

(A) Ins(1,3,4)P_3 as observed in the structure. Contact sites for phosphate and hydroxyl groups are marked by colored ovals.

(B) Predicted orientation of Ins(3,4,5,6)P_3.

(C) Predicted orientation of Ins(1,2,4)P_3.

(D) Predicted orientation of Ins(1,4,5)P_3.

this enzyme is able to phosphorylate its substrate by a direct inline transfer of the ATP γ-phosphate to either the 5 or 6 hydroxyl of Ins(1,3,4)P_3.

In addition to its 5/6-kinase activity, IP56K interconverts Ins(1,3,4,5)P_4 and Ins(1,3,4,6)P_4 in a "mutase" reaction (Figure 5) (Ho et al., 2002), and has been reported to have a phosphatase activity which reverses the kinase reaction (Ho et al., 2002). We find that under the conditions of crystallization and in the presence of Mg^{2+} and ADP, Ins(1,3,4,5)P_4 is converted to Ins(1,3,4,6)P_4. Two mechanisms are possible for these reactions. One involves the back reaction of the kinase, followed by ATP hydrolysis in the case of the phosphatase activity, or phosphorylation of the alternative hydroxyl group in the case of the mutase activity. The second would involve the formation of a covalent phosphoenzyme intermediate in a manner that required the presence of ADP. In this scenario, that ADP would be required for catalysis but would not itself undergo any reaction. The role for the ADP in this scenario might be to coordinate the catalytic Mg^{2+} ions. The Nδ of His-147 is 3.0 Å away from the AMPPCP γ-phosphate (Figure 3B), and it is tempting to speculate that it could be covalently phosphorylated. There is no other reactive amino acid residue close enough to the γ-phosphate to be a reasonable candidate for a transient phosphorylation site. At least two other ATP-grasp proteins go through phosphohistidine intermediates (Herzberg et al., 1996; Wolodko et al., 1994). The human counterpart of His-147 is His-167. The human H167A mutant retains detectable catalytic activity at about 0.03% of wild-type levels. The presence of residual activity in the H167A mutant argues that this His has an important role in catalysis, but is not involved in an obligate phosphoenzyme intermediate.

Structural Determinants for Substrate Specificity

The structure of the enzyme-substrate complex shows that phosphate groups, rather than hydroxyl groups, dictate substrate binding. Thus the details of the stereochemistry of each position of the ring matter less for binding than the overall arrangement of phosphate groups. To consider possible allowed binding modes for alternative substrates, the subsite in which the Ins(1,3,4)P_3 6-hydroxyl binds was designated position A. The other sites are designated clockwise B through F (Figure 6A). The first requirement for IP phosphorylation is that free hydroxyl groups occupy sites A and B. Secondly, phosphates should be present in sites C, D, and F. Site E binds the free 2-hydroxyl in the Ins(1,3,4)P_3 complex. The 2-hydroxyl projects toward solution and has no interactions with the enzyme. Site E therefore can be occupied by a free hydroxyl or by a phosphate group.

Twelve unique inositol phosphates are predicted to be substrates by considering all possible rotations about an axis normal to the inositol ring (Table S1 in the Supplemental Data available with this article online). Of these only one other than Ins(1,3,4)P_3 is a documented physiological substrate: Ins(3,4,5,6)P_4 (Tan et al., 1997; Yang et al., 1999). If a rotation about an axis through the 1 and 4 positions is considered in addition to rotations about an axis through the ring, another six trisphosphate substrates are predicted. No additional tetrakisphosphate substrates or reactions are predicted by this operation, which simply interchanges the two phosphate groups occupying sites D and E with each other, and the two hydroxyls occupying sites A and B with each other. Three of the potential trisphosphate substrates have been tested. Ins(1,4,5)P_3 is a substrate of the *E. histolytica* enzyme under first order rate conditions, although it is not a physiological substrate for the human enzyme (Field et al., 2000). Subtle differences in active site residues between the *E. histolytica* and human enzymes, such as the replacement of Ser-295 in the former by a Gly in the latter, appear to drive these specificity differences (Figures 2A and 6). The presumed nonphysiological compounds Ins(1,2,4)P_3 (Adelt et al., 2001) and Ins(3,4,6) P_3 (Ho et al., 2002) are both substrates of the human enzyme.

The structure of IP56K provides a unifying framework in which to consider the exceptionally wide range of activities attributed to it. Protein kinase activity has been observed to copurify with IP56K purified from insect cells (Wilson et al., 2001). The constricted active site of IP56K is typical of a small-molecule modifying enzyme, and it is difficult to model binding of a peptide substrate. Structural analysis suggests that IP56K is

unlikely to be a protein kinase. The constriction of the active site explains the absence of lipid phosphoinositide activity, as seen also in the structure of Ins(1,4,5)P_3 3-kinase (Gonzalez et al., 2004; Miller and Hurley, 2004). In summary, the structure shows how the ATP-grasp fold of IP56Ks from both *E. histolytica* and humans is well adapted to its function as a multifunctional small molecule kinase and isomerase.

Experimental Procedures

Expression, Purification, and Crystallization of *E. histolytica* IP56K

The full-length (aa1-319) Ins(1,3,4)P_3 5/6-kinase from *E. histolytica* was expressed as a GST-tagged fusion protein in *Escherichia coli* strain Rosetta (DE3) (Novagen). The expressed fusion was purified by affinity chromatography using glutathione-Sepharose (GE-Pharmacia). The column was washed with 10 column volumes of 10 mM Na phosphate (pH 7.4) and 150 mM NaCl follwed by 10 column volumes of 10 mM Na phosphate (pH 7.4) and 500 mM NaCl. The fusion protein was eluted in 10 mM Na phosphate, 150 mM NaCl and 50 mM glutathione. During dialysis, the GST tag was removed by cleavage with PreScission protease (GE-Pharmacia). The protein was subjected to a second purification using a glutathione-Sepharose column. Following concentration, ammonium sulfate was added to a final concentration of 1.1 M and the protein was purified on a PHE15 SOURCE column (GE-Pharmacia) and eluted over a gradient of decreasing ammonium sulfate concentration followed by an increasing glycerol concentration gradient to a final concentration of 40%. Following dialysis, the protein was further purified using a Superdex 200 26/60 gel filtration column (GE-Pharmacia) equilibrated with 25 mM Tris-HCl (pH 8.0), 150 mM NaCl and 10 mM DTT. Initial crystallization trials were performed at 30 mg/ml protein. Crystals which diffracted to 6 Å in 20% PEG 3000, 0.1 M Tris-HCl (pH 7.5) and 0.1 M $Ca(OAc)_2$ grew over the course of several months. Seeding of these crystals into a preequilibrated sitting drop of 15 mg/m1 protein, 25% PEG 3350, 5% PEG 400, 0.1 M bis-tris (pH 5.5), 10 mM DTT, 10 mM L-cysteine, 10 mM AMPPNP, 10 mM $MgCl_2$ and 5 mM Ins(1,3,4)P_3 produced crystals which diffracted to 2 Å. Further seeding of these crystals into 25% PEG 3350, 0.1 M bis-tris (pH 5.5) and 10 mM DTT with added ligands, including inositol compounds, and ADP, produced crystals in space group $P2_1$ with cell dimensions a = 38.2 Å, b = 94.8 Å, c= 47.4 Å, β = 110.4°, that diffracted to up to 1.2 Å resolution. To obtain the AMPPCP complex, crystals grown in the presence on Ins(1,3,4)P_3 and $MgCl_2$ were soaked in 20 mM AMPPCP.

X-Ray Data Collection and Structure Determination

One two-wavelength multiwavelength anomalous dispersion (MAD) data set was collected of crystals cocrystallized with $Sm(OAc)_3$ (Table 1, Sm1 and Sm2) at beamline 8.2.1, 1 Lawrence Berkeley National Laboratory, and one four-wavelength MAD data set was collected of crystals soaked in $HgCl_2$ (Table 1, Hg1- Hg4) at beamline X-25, Brookhaven National Laboratory. Data were processed with HKL2000 (HKL Research). One Sm and three Hg sites were located with SOLVE (Terwilliger and Berendzen, 1999), and the figure of merit for this solution was 0.59. Phase extension was performed to 1.2 Å in RESOLVE (Terwilliger, 2000) using native data collected at SSRL. The initial 210 residues were traced automatically using ARP/wARP (Perrakis et al., 1999). The 1.2 Å map was further interpreted using O (Jones et al., 1991). Refinement was carried out initially using torsional dynamics in CNS (Brunger et al., 1998) and refmac5 (Murshudov et al., 1997). Electron density maps were generated for the native datasets of other combinations of ligands in CNS. Native datasets of the binary complex and ternary complexes of Ins(1,3,4)P_3 and Ins(1,3,4,6)P_4 were collected at beamline 9-2, Stanford Synchrotron Radiation Laboratory; beamline X26, Brookhaven National Laboratory; beamline 8.2.1 Lawrence Berkeley National Laboratory; and beamline 22-BM, Advanced Photon Source, respectively.

Homology Modeling of Human IP56K

A homology model of the human IP56K was created by using Swiss-Model and was energy minimized using SwissPDB Viewer. An alignment of the *E. histolytica* and *H. sapiens* protein sequences was created using T-COFFEE (Notredame et al., 2000), and was manually edited and threaded into the *E. histolytica* structure using SwissPDB Viewer (Schwede et al., 2003).

Site-Directed Mutagenesis

Mutagenesis was performed using pBacPAK9-human 5/6-kinase as template (Wilson et al., 2001) and the QuikChange Site-directed Mutagenesis kit (Stratagene) according to manufacturer's instructions. Mutagenesis was confirmed by sequencing constructs using the ABI prizm Big Dye terminator (PerkinElmer Life Sciences).

Expression and Purification of Human IP56K

Sf9 cells were grown in serum-free medium (Invitrogen) in suspension culture. Transfections were done with Bacfectin and BacPAK6 DNA (BD Biosciences). For protein production, 300 ml cultures were infected with the appropriate virus for three days. Cells were harvested and frozen as pellets at –80°C until use. Pellets were resuspended in 30–50 ml homogenization buffer consisting of 20 mM HEPES, (pH 7.6), 140 mM NaCl, 10% glycerol, 0.1% NP40, 10 mM benzamidine, 40 μM iodoacetamide, 1 μM pepstatin A, 40 μM leupeptin, 10 μM bestatin, 50 μg chymostatin/ml μM calpain inhibitor, 1 μM microcystin, 1 mM PMSF, and 1 mM sodium ortho-vanadate. Following a freeze-thaw cycle on dry ice, extracts were sonicated briefly, Dnase I (Sigma) was added to a final concentration of 10 μg/ml, and extracts were allowed to sit on ice for 30 min. Extracts were clarified by filtration and applied to a 1 ml anti-FLAG® M2-agarose affinity gel (Sigma) equilibrated in TBS. Following extensive washing with TBS, protein was eluted with Flag peptide (Sigma, 100 μg/ml). Fractions containing protein were pooled and dialyzed against TBS containing 1 mM DTT and 3 mM $MgCl_2$. Protein concentrations were determined using the Bio-Rad protein assay reagent (Bio-Rad). Purified, dialyzed protein was stored at –80°C in aliquots until use.

Production and Separation of Inositol Polyphosphates

[^{3}H]inositol 1,3,4-trisphosphate was produced from [^{3}H]inositol 1,3,4,5-tetrakisphosphate (PerkinElmer Life Sciences) as described (Wilson et al., 2001). [^{3}H]inositol 1,3,4,6-tetrakisphosphate was prepared as previously described (Chang et al., 2002). Preparation of [^{32}P]inositol 1,3,4,5-tetrakisphosphate (Wilson and Majerus, 1996) and [^{32}P]InsP_6 (Verbsky et al., 2005) were described previously. [^{3}H]inositol 1,4,5,6 tetrakisphosphate was a generous gift from Shao-Chun Chang. Separation of soluble inositol polyphosphates was done as described (Wilson and Majerus, 1996).

Enzyme Assays

Ins(1,3,4)P_3 5/6-kinase assays were done as described, except for the absence of $LiCl_2$ in the assay mix (Wilson and Majerus, 1996). Enzyme was diluted in buffer containing 20 mM HEPES, (pH 7.2), 1 mM ATP, 6 mM $MgCl_2$, 100 mM KCl, 1 mM DTT, and 100 μg BSA/ml. Assays for isomerization of the inositol tetrakisphosphate species were done in a reaction volume of 100 μl in the same buffer as that for Ins(1,3,4)P_3 5/6-kinase assays, with the substrate being 3000 cpm of either [^{3}H]inositol 1,3,4,5-tetrakisphosphate or [^{3}H]-inositol 1,3,4,6-tetrakisphosphate. Due to the low inositol kinase activity of many of the point mutants, isomerase assays were allowed to proceed for 3 hr at 37°C to ensure that equilibrium had been reached.

Supplemental Data

Supplemental Data include an additional table and can be found with this article online at http://www.molecule.org/cgi/content/full/18/2/201/DC1/.

Acknowledgments

We thank Bertram Canagarajah and Hang Shi for assistance with data collection, Fred Dyda for home source X-ray facility support

and comments on the manuscript, and Salvatore Sechi for assistance with mass spectrometry. J.H.H. thanks Stephen Shears for helpful discussions. We thank the staffs of beamlines X25 and X26, National Synchrotron Light Source (NSLS), Brookhaven National Laboratory (BNL), 9-2 Stanford Synchrotron Radiation Laboratory (SSRL), 8.2.1 Advanced Light Source (ALS), Lawrence Berkeley National Laboratory (LBL), and 22-BM, Advanced Photon Source (APS), and Argonne National Laboratory (ANL) for assistance with X-ray data collection and for access to beam time. This research was supported by NIDDK intramural support to J.H.H. and National Institutes of Health (NIH) grants R01-HL016634-39 and R01-HL55672-09 to P.W.M. Research carried out at the NSLS, BNL, was supported by the United States Department of Energy (DOE), Division of Materials Sciences and Division of Chemical Sciences, under Contract No. DE-AC02-98CH10886. The ALS is supported by the Director, Office of Science, Office of Basic Energy Sciences, Materials Sciences Division, of the U.S. DOE under Contract No. DE-AC03-76SF00098 at LBL. The SSRL, a national user facility operated by Stanford University on behalf of the U.S. DOE, Office of Basic Energy Sciences, is supported by the DOE, Office of Biological and Environmental Research, and by the NIH, National Center for Research Resources, Biomedical Technology Program, and the National Institute of General Medical Sciences. Use of the APS was supported by the U.S. DOE, Basic Energy Sciences, Office of Science, under Contract No.W-31-109-Eng-38.

Received: February 2, 2005
Revised: March 10, 2005
Accepted: March 18, 2005
Published: April 14, 2005

References

Abel, K., Anderson, R.A., and Shears, S.B. (2001). Phosphatidylinositol and inositol phosphate metabolism. J. Cell Sci. *114*, 2207–2208.

Adelt, S., Plettenburg, O., Dallmann, G., Ritter, F.P., Shears, S.B., Altenbach, H.J., and Vogel, G. (2001). Regiospecific phosphohydrolases from Dictyostelium as tools for the chemoenzymatic synthesis of the enantiomers D-myo-inositol 1,2,4-trisphosphate and D-myo-inositol 2,3,6-trisphosphate: Non-physiological, potential analogues of biologically active D-myo-inositol 1,3,4-trisphosphate. Bioorg. Med. Chem. Lett. *11*, 2705–2708.

Artymiuk, P.J., Poirrette, A.R., Rice, D.W., and Willett, P. (1996). Biotin carboxylase comes into the fold. Nat. Struct. Biol. *3*, 128–132.

Brunger, A.T., Adams, P.D., Clore, G.M., DeLano, W.L., Gros, P., Grosse-Kunstleve, R.W., Jiang, J.S., Kuszewski, J., Nilges, M., Pannu, N.S., et al. (1998). Crystallography & NMR system: A new software suite for macromolecular structure determination. Acta Crystallogr. D Biol. Crystallogr. *54*, 905–921.

Chang, S.C., Miller, A.L., Feng, Y., Wente, S.R., and Majerus, P.W. (2002). The human homolog of the rat inositol phosphate multikinase is an inositol 1,3,4,6-tetrakisphosphate 5-kinase. J. Biol. Chem. *277*, 43836–43843.

Cheek, S., Zhang, H., and Grishin, N.V. (2002). Sequence and structure classification of kinases. J. Mol. Biol. *320*, 855–881.

Efanov, A.M., Zaitsev, S.V., and Berggren, P.O. (1997). Inositol hexakisphosphate stimulates non-Ca2+-mediated and primes Ca2+-mediated exocytosis of insulin by activation of protein kinase C. Proc. Natl. Acad. Sci. USA *94*, 4435–4439.

Esser, L., Wang, C.R., Hosaka, M., Smagula, C.S., Sudhof, T.C., and Deisenhofer, J. (1998). Synapsin I is structurally similar to ATP-utilizing enzymes. EMBO J. *17*, 977–984.

Fan, C., Moews, P.C., Shi, Y., Walsh, C.T., and Knox, J.R. (1995). A Common Fold for Peptide Synthetases Cleaving Atp to Adp - Glutathione Synthetase and D-Alanine-D-Alanine Ligase of Escherichia-Coli. Proc. Natl. Acad. Sci. USA *92*, 1172–1176.

Fan, C., Moews, P.C., Walsh, C.T., and Knox, J.R. (1994). Vancomycin Resistance - Structure of D-Alanine-D-Alanine Ligase at 2.3-Angstrom Resolution. Science *266*, 439–443.

Field, J., Wilson, M.P., Mai, Z.M., Majerus, P.W., and Samuelson, J. (2000). An Entamoeba histolytica inositol 1,3,4-trisphosphate 5/6-kinase has a novel 3-kinase activity. Mol. Biochem. Parasitol. *108*, 119–123.

Galperin, M.Y., and Koonin, E.V. (1997). A diverse superfamily of enzymes with ATP-dependent carboxylate-amine/thiol ligase activity. Protein Sci. *6*, 2639–2643.

Gonzalez, B., Schell, M.J., Letcher, A.J., Veprintsev, D.B., Irvine, R.F., and Williams, R.L. (2004). Structure of a human inositol 1,4,5-trisphosphate 3-kinase: Substrate binding reveals why it is not a phosphoinositide 3-kinase. Mol. Cell *15*, 689–701.

Hanakahi, L.A., Bartlet-Jones, M., Chappell, C., Pappin, D., and West, S.C. (2000). Binding of inositol phosphate to DNA-PK and stimulation of double-strand break repair. Cell *102*, 721–729.

Hanakahi, L.A., and West, S.C. (2002). Specific interaction of IP6 with human Ku70/80, the DNA-binding subunit of DNA-PK. EMBO J. *21*, 2038–2044.

Herzberg, O., Chen, C.C.H., Kapadia, G., McGuire, M., Carroll, L.J., Noh, S.J., and Dunaway-Mariano, D. (1996). Swiveling-domain mechanism for enzymatic phosphotransfer between remote reaction sites. Proc. Natl. Acad. Sci. USA *93*, 2652–2657.

Ho, M.W.Y., Yang, X.N., Carew, M.A., Zhang, T., Hua, L., Kwon, Y.U., Chung, S.K., Adelt, S., Vogel, G., Riley, A.M., et al. (2002). Regulation of Ins(3,4,5,6)P-4 signaling by a reversible kinase/phosphatase. Curr. Biol. *12*, 477–482.

Holm, L., and Sander, C. (1995). Dali - a Network Tool for Protein-Structure Comparison. Trends Biochem. Sci. *20*, 478–480.

Hoy, M., Berggren, P.O., and Gromada, J. (2003). Involvement of protein kinase C-epsilon in inositol hexakisphosphate-induced exocytosis in mouse pancreatic beta-cells. J. Biol. Chem. *278*, 35168–35171.

Irvine, R.F., and Schell, M.J. (2001). Back in the water: The return of the inositol phosphates. Nat. Rev. Mol. Cell Biol. *2*, 327–338.

Jones, T.A., Zou, J.Y., Cowan, S.W., and Kjeldgaard, A. (1991). Improved methods for building protein models in electron density maps and the location of errors in these models. Acta Crystallogr. D Biol. Crystallogr. *47*, 110–119.

Kourie, J.I., Foster, P.S., and Dulhunty, A.F. (1997). Inositol polyphosphates modify the kinetics of a small chloride channel in skeletal muscle sarcoplasmic reticulum. J. Membr. Biol. *157*, 147–158.

Larsson, O., Barker, C.J., Sjoholm, A., Carlqvist, H., Michell, R.H., Bertorello, A., Nilsson, T., Honkanen, R.E., Mayr, G.W., Zwiller, J., and Berggren, P.O. (1997). Inhibition of phosphatases and increased Ca2+ channel activity by inositol hexakisphosphate. Science *278*, 471–474.

Luo, H.R., Huang, Y.E., Chen, J.C., Saiardi, A., Iijima, M., Ye, K., Huang, Y., Nagata, E., Devreotes, P., and Snyder, S.H. (2003). Inositol pyrophosphates mediate chemotaxis in Dictyostelium via pleckstrin homology domain-PtdIns(3,4,5)P3 interactions. Cell *114*, 559–572.

Majerus, P.W., Kisseleva, M.V., and Norris, F.A. (1999). The role of phosphatases in inositol signaling reactions. J. Biol. Chem. *274*, 10669–10672.

Michell, R.H. (2002). Inositol phosphates: A remarkably versatile enzyme. Curr. Biol. *12*, R313–R315.

Miller, G.J., and Hurley, J.H. (2004). Crystal structure of the catalytic core of inositol 1,4,5-trisphosphate 3-kinase. Mol. Cell *15*, 703–711.

Murshudov, G.N., Vagin, A.A., and Dodson, E.J. (1997). Refinement of macromolecular structures by the maximum-likelihood method. Acta Crystallogr. D Biol. Crystallogr. *53*, 240–255.

Notredame, C., Higgins, D., and Heringa, J. (2000). T-Coffee: A novel method for multiple sequence alignments. J. Mol. Biol. *302*, 205–217.

Odom, A.R., Stahlberg, A., Wente, S.R., and York, J.D. (2000). A role for nuclear inositol 1,4,5-trisphosphate kinase in transcriptional control. Science *287*, 2026–2029.

Perrakis, A., Morris, R., and Lamzin, V.S. (1999). Automated protein model building combined with iterative structure refinement. Nat. Struct. Biol. *6*, 458–463.

Pouillon, V., Hascakova-Bartova, R., Pajak, B., Adam, E., Bex, F.,

Dewaste, V., Van Lint, C., Leo, O., Erneux, C., and Schurmans, S. (2003). Inositol 1,3,4,5-tetrakisphosphate is essential for T lymphocyte development. Nat. Immunol. *4*, 1136–1143.

Saiardi, A., Erdjument-Bromage, H., Snowman, A.M., Tempst, P., and Snyder, S.H. (1999). Synthesis of diphosphoinositol pentakisphosphate by a newly identified family of higher inositol polyphosphate kinases. Curr. Biol. *9*, 1323–1326.

Saiardi, A., Bhandari, R., Resnick, A.C., Snowman, A.M., and Snyder, S.H. (2004). Phosphorylation of protein by inositol pyrophosphates. Science *306*, 2101–2105.

Saiardi, A., Resnick, A.C., Snowman, A.M., Wendland, B., and Snyder, S.H. (2005). Inositol pyrophosphates regulate cell death and telomere length through phosphoinositide 3-kinase-related protein kinases. Proc. Natl. Acad. Sci. USA *102*, 1911–1914.

Sakai, H., Vassylyeva, M.N., Matsuura, T., Sekine, S., Gotoh, K., Nishiyama, M., Terada, T., Shirouzu, M., Kuramitsu, S., Vassylyev, D.G., and Yokoyama, S. (2003). Crystal structure of a lysine biosynthesis enzyme, LysX, from Thermus thermophilus HB8. J. Mol. Biol. *332*, 729–740.

Schwede, T., Kopp, J., Guex, N., and Peitsch, M.C. (2003). SWISS-MODEL: an automated protein homology-modeling server. Nucleic Acids Res. *31*, 3381–3385.

Shears, S.B. (2004). How versatile are inositol phosphate kinases? Biochem. J. *377*, 265–280.

Shen, X., Xiao, H., Ranallo, R., Wu, W.H., and Wu, C. (2003). Modulation of ATP-dependent chromatin-remodeling complexes by inositol polyphosphates. Science *299*, 112–114.

Steger, D.J., Haswell, E.S., Miller, A.L., Wente, S.R., and O'Shea, E.K. (2003). Regulation of chromatin remodeling by inositol polyphosphates. Science *299*, 114–116.

Streb, H., Irvine, R.F., Berridge, M.J., and Schulz, I. (1983). Release of Ca2+ from a nonmitochondrial intracellular store in pancreatic acinar cells by inositol-1,4,5-trisphosphate. Nature *306*, 67–69.

Tan, Z., Bruzik, K.S., and Shears, S.B. (1997). Properties of the inositol 3,4,5,6-tetrakisphosphate 1-kinase purified from rat liver—Regulation of enzyme activity by inositol 1,3,4-trisphosphate. J. Biol. Chem. *272*, 2285–2290.

Terwilliger, T.C. (2000). Maximum-likelihood density modification. Acta Crystallogr. D Biol. Crystallogr. *56*, 965–972.

Terwilliger, T.C., and Berendzen, J. (1999). Automated MAD and MIR structure solution. Acta Crystallogr. D Biol. Crystallogr. *55*, 849–861.

Thoden, J.B., Firestine, S., Nixon, A., Benkovic, S.J., and Holden, H.M. (2000). Molecular structure of Escherichia coli PurT-encoded glycinamide ribonucleotide transformylase. Biochemistry *39*, 8791–8802.

Thoden, J.B., Kappock, T.J., Stubbe, J., and Holden, H.M. (1999). Three-dimensional structure of N-5-carboxyaminoimidazole ribonucleotide synthetase: A member of the ATP-grasp protein superfamily. Biochemistry *38*, 15480–15492.

Verbsky, J.W., Chang, S.C., Wilson, M.P., Mochizuki, Y., and Majerus, P.W. (2005). The pathway for the production of inositol hexakisphosphate (InsP6) in human cells. J. Biol. Chem. *280*, 1911–1920.

Wilson, M.P., and Majerus, P.W. (1996). Isolation of inositol 1,3,4-trisphosphate 5/6-kinase, cDNA cloning, and expression of the recombinant enzyme. J. Biol. Chem. *271*, 11904–11910.

Wilson, M.P., Sun, Y., Cao, L., and Majerus, P.W. (2001). Inositol 1,3,4-trisphosphate 5/6-kinase is a protein kinase that phosphorylates the transcription factors c-Jun and ATF-2. J. Biol. Chem. *276*, 40998–41004.

Wolodko, W.T., Fraser, M.E., James, M.N.G., and Bridger, W.A. (1994). The Crystal-Structure of Succinyl-Coa Synthetase from Escherichia-Coli at 2.5-Angstrom Resolution. J. Biol. Chem. *269*, 10883–10890.

Yang, X.N., Rudolf, M., Carew, R.A., Yoshida, M., Nerreter, V., Riley, A.M., Chung, S.K., Bruzik, K.S., Potter, B.V.L., Schultz, C., and Shears, S.B. (1999). Inositol 1,3,4-trisphosphate acts in vivo as a specific regulator of cellular signaling by inositol 3,4,5,6-tetrakisphosphate. J. Biol. Chem. *274*, 18973–18980.

York, J.D., Guo, S.L., Odom, A.R., Spiegelberg, B.D., and Stolz, L.E. (2001). An expanded view of inositol signaling. Adv. Enzyme Regul. *41*, 57–71.

York, J.D., Odom, A.R., Murphy, R., Ives, E.B., and Wente, S.R. (1999). A phospholipase C-dependent inositol polyphosphate kinase pathway required for efficient messenger RNA export. Science *285*, 96–100.

York, S.J., Armbruster, B.N., Greenwell, P., Peters, T.D., and York, J.D. (2005). Inositol diphosphate signaling regulates telomere length. J. Biol. Chem. *285*, 96–100. in press.

Accession numbers

Structural coordinates have been deposited in the Protein Data Bank with accession numbers 1Z2N, 1Z2O, and 1Z2P.

Supplemental Data

Specificity Determinants in Inositol Polyphosphate Synthesis: Crystal Structure of Inositol 1,3,4-Trisphosphate 5/6-Kinase

Gregory J. Miller, Monita P. Wilson, Philip W. Majerus, and James H. Hurley

Table S1. Theoretically Possible Inositol Substrates

Ring normal Substrate	Site (A,B)	*1,4 axis* Substrate	Site (A,B)
1,3,4	**6,5**	**1,4,5**	2,**3**[a]
1,2,3,4	6,5		5,6
2,4,5	1,6	2,5,6	3,4
2,3,4,5	1,6		6,1
3,5,6	2,1	1,3,6	4,5
3,4,5,6	~~2~~,**1**		**1**,~~2~~
1,4,6	3,2	**1,2,4**	**5**,6[b]
1,4,5,6	3,2		2,3
1,2,5	4,3	2,3,5	6,1
1,2,5,6	4,3		3,4
~~2,3,6~~	~~5,4~~	**3,4,6**	**1**,~~2~~
1,2,3,6	5,4		4,5

Known substrates and phosphorylation sites are indicated in bold type. Compounds known to be non-substrates and sites known to be nonreactive are shown in struck-out type.

[a]This reaction is observed for the amoeba but only at trace levels for the human enzyme.
[b]7 % of the product is phosphorylated at the 6-position.